Cell

Virus Infection Induces NF-κB-Dependent Interchromosomal Associations Mediating Monoallelic *IFN-β* Gene Expression

Effie Apostolou[1] and Dimitris Thanos[1,*]
[1]Institute of Molecular Biology, Genetics and Biotechnology, Biomedical Research Foundation, Academy of Athens, 4 Soranou Efesiou Street, Athens 11527, Greece
*Correspondence: thanos@bioacademy.gr
DOI 10.1016/j.cell.2008.05.052

SUMMARY

Transcriptional activation of the *IFN-β* gene by virus infection requires the cooperative assembly of an enhanceosome. We report that the stochastic and monoallelic expression of the IFN-β gene depends on interchromosomal associations with three identified distinct genetic loci that could mediate binding of the limiting transcription factor NF-κB to the *IFN-β* enhancer, thus triggering enhanceosome assembly and activation of transcription from this allele. The probability of a cell to express IFN-β is dramatically increased when the cell is transfected with any of these loci. The secreted IFN-β protein induces high-level expression of the enhanceosome factor IRF-7, which in turn promotes enhanceosome assembly and *IFN-β* transcription from the remaining alleles and in other initially nonexpressing cells. Thus, the *IFN-β* enhancer functions in a nonlinear fashion by working as a signal amplifier.

INTRODUCTION

The human antiviral response is triggered by the transcriptional activation of type I interferon genes (20 *IFN-α*, 5 *IFN-ω*, and 1 *IFN-β*) (Paun and Pitha, 2007; Taniguchi and Takaoka, 2002). This leads to the production and secretion of IFN proteins that bind to type I IFN receptors on the surface of both infected and uninfected cells, leading to the expression of a large number of antiviral genes (Stetson and Medzhitov, 2006). Transcriptional activation of the human *IFN-β* gene requires an enhancer element located immediately upstream of the core promoter. The *IFN-β* enhancer is recognized by three distinct sets of transcription factors (NF-κB, IRFs, and ATF-2/cJun) and by the architectural protein HMGI(Y). Virus infection leads to the coordinate activation of all three types of transcription factors, which assemble on the IFN enhancer to form a multiprotein complex known as the *IFN-β* enhanceosome (Thanos and Maniatis, 1995). Enhanceosome assembly occurs only after viral infection and not in response to other signals that can separately activate each of the transcription factors (Thanos and Maniatis, 1995; Lomvardas and Thanos, 2002). This combinatorial mechanism is based on the fact that virus infection is the only known signal that can activate all of the *IFN-β* transcriptional activators simultaneously (Maniatis et al., 1998; Munshi et al., 1999). Following its assembly on the nucleosome-free enhancer, the enhanceosome instructs the ordered recruitment of chromatin modifiers and basal transcription factors to the nearby promoter (Agalioti et al., 2000). This recruitment program culminates with sliding of a nucleosome masking the core promoter, thus allowing the binding of RNA polymerase II and the initiation of transcription (Lomvardas and Thanos, 2001).

The cooperative assembly of the enhanceosome and the organization of nucleosomes in the enhancer/promoter region ensure a high degree of specificity in the transcriptional response. Thus, aberrant transcription from individual transcription factors that are each activated by a variety of other signals (TNF-α, IFNs, stress, etc.) is prevented (Lomvardas and Thanos, 2002). Previous biochemical and structure determination experiments revealed an unexpected complexity in the mechanisms driving enhanceosome assembly. Chromatin immunoprecipitation experiments revealed a stepwise assembly of the enhanceosome (Munshi et al., 2001; Lomvardas and Thanos, 2002). More specifically, NF-κB is initially detected at the IFN-β enhancer at 2 hr after virus infection together with IRF-1, whereas ATF-2 is recruited to the enhancer an hour later followed by the arrival of IRF-3 and c-Jun. IRF-7 is incorporated into the enhanceosome just before initiation of transcription (5–6 hr post-infection). The enhanceosome remains intact for 6 additional hours, and this correlates with the peak of transcriptional activation.

The three-dimensional structure of the intact enhanceosome, as deduced from the assembly of separate structures of pairs of transcription factors bound to their sites, revealed that cooperative assembly derives from binding-induced changes in DNA conformation and to a lesser extent from protein-protein interactions (Escalante et al., 2007; Panne et al., 2007). This observation is in agreement with the stepwise assembly of the enhanceosome in vivo (Munshi et al., 2001), during which the sequential arrival of transcription factors onto the enhancer alters the DNA structure, thus allowing the subsequent binding of the nearby factors.

A striking feature of *IFN-β* expression (Zawatzky et al., 1985; Enoch et al., 1986; Senger et al., 2000; Hu et al., 2007), as well as of many other cytokine genes, including *IL-2* (Holländer et al., 1998), *IL-4* (Riviere et al., 1998), *IL-5* (Kelly and Locksley,

2000), *IL-13* (Kelly et Locksley, 2000; Guo et al., 2005), and *IL-10* (Calado et al., 2006), is that, even under optimal conditions, only a fraction of the cells in the population expresses the cytokine gene at any given moment. This heterogeneity is not due to mixed populations of producing and nonproducing cells but rather is a stochastic phenomenon, as revealed by cell cloning experiments (Zawatzky et al., 1985). An additional characteristic of cytokine gene expression is that gene activation is predominantly monoallelic, thus further underscoring the stochastic mode of gene regulation. A recent study applying single cell RT-PCR analysis and stochastic model simulation provided initial evidence for allelic imbalance of virus-induced *IFN-β* gene transcription (Hu et al., 2007). However, the mechanisms of stochastic *IFN-β* gene expression and allelic imbalance remain elusive.

What transcription mechanism can assure the random choice of cells expressing IFN-β after virus infection? One attractive model invokes the transcription process itself and therefore is likely associated with the inherent complexity of enhanceosome assembly on the *IFN-β* enhancer/promoter. Since enhanceosome assembly is a cooperative process, we asked whether limiting concentrations of one or some of the *IFN-β* activators accounts for the stochastic assembly of enhanceosomes thus leading to binary transcriptional switches. We present evidence for a model in which virus infection induces the stochastic expression of the *IFN-β* gene from a single allele in a small population of cells. The choice of the allele to be expressed depends on interchromosomal associations with three identified distinct genetic loci that could mediate binding of the limiting transcription factor NF-κB to the *IFN-β* enhancer promoting enhanceosome assembly and activation of transcription from this allele. The secreted IFN-β protein induces high-level expression of the enhanceosome factor IRF-7, which in turn promotes enhanceosome assembly and *IFN-β* transcription from the remaining alleles and in other initially nonexpressing cells. Thus, the *IFN-β* enhancer functions in a nonlinear fashion and works as a signal amplifier.

RESULTS

Limiting Amounts of NF-κB and IRF Proteins Contribute to the Stochastic Expression of the *IFN-β* Gene

To investigate whether individual enhanceosome components are present in cells at suboptimal concentrations, we transfected HeLa cells with expression vectors producing each of the *IFN-β* activators, followed by virus infection for 6 hr and hybridization with an antisense *IFN-β* digoxigenin-labeled RNA probe. Control experiments using GFP reporters have indicated that under our conditions approximately 90% of HeLa cells can be transfected (data not shown). Figures 1A and 1B show that only 20% of the cells in the population transcribe the *IFN-β* gene in response to virus infection, a result consistent with previous studies (Zawatzky et al., 1985; Enoch et al., 1986; Senger et al., 2000; Hu et al., 2007). Remarkably, the percentage of IFN-β-producing cells after virus infection increases to 75%, when the cells were transfected with an expression vector producing the p65 subunit of NF-κB and to 55% after IRF-7 expression. Smaller increases were observed when either ATF-2/cJun, IRF-1, or IRF-3 were expressed, whereas increasing the concentration of HMGI(Y) did not affect the number of cells expressing IFN-β (Figures 1A and 1B). In control experiments we showed that hybridization with a sense *IFN-β* RNA probe did not produce a signal (data not shown). The increase in the number of IFN-β-producing cells is also reflected in the amount of total *IFN-β* mRNA produced, as seen by the RT-PCR experiment shown in Figure 1C. These experiments suggest that NF-κB, IRF-7, IRF-3, and to a lesser extent ATF-2/cJun and IRF-1 exist at suboptimal concentrations within the cells and the failure of some cells to express IFN-β can be bypassed by increasing the cellular concentration of these proteins. The increase of IFN-β-expressing cells is not observed in uninfected cells (not shown), indicating that overexpression of these factors did not bypass the requirement for enhanceosome assembly after virus infection. To test whether NF-κB overexpression increases not only the percentage of IFN-β-expressing cells but also the amount of *IFN-β* mRNA produced per cell, we carried out the experiment shown in Figure 1D. HeLa cells were transfected with the NF-κB expression vector along with a GFP vector and the cells were either mock or virus infected. GFP-positive cells were isolated by cell sorting, and the amount of *IFN-β* mRNA was determined by real-time RT-PCR. As seen in the figure, the increase in *IFN-β* mRNA production (4.1-fold) is similar to the increase of the number of cells (3.5-fold) producing *IFN-β* expression following NF-κB overexpression (Figure 1B). Thus, the *IFN-β* expression levels per cell are not significantly affected by NF-κB overexpression.

Virus Infection Induces Colocalization of the *IFN-β* Gene with Three Distant NF-κB Bound Genomic Loci

The low concentration of NF-κB within cells (approximately 50.000 molecules, Hottiger et al., 1998; Lipniacki et al., 2006; and our unpublished data) when taken together with the fact that it is the first factor that binds to the *IFN-β* promoter (Munshi et al., 2001) poses a major question regarding the mechanism by which NF-κB locates the *IFN-β* gene and nucleates enhanceosome assembly in the context of the human genome. We hypothesized that there exist "specialized" NF-κB sites that might be capable of interacting with NF-κB immediately and preferentially after its entry into the nucleus. Next, NF-κB could associate with the promoters of target genes via inter- and/or intrachromosomal interactions, thus "delivering" the factor to the correct site. Since interchromosomal interactions are stochastic in nature (de Laat and Grosveld, 2007; Misteli 2007), such a model could explain some of the features of *IFN-β* expression discussed above. To test this idea we employed circular chromosome conformation capture (4C) (Ling et al., 2006; Zhao et al., 2006) coupled with chromatin immunoprecipitation (Figure 2A). The 4C method is based on the proximity ligation principle, in which DNA-protein complexes existing in *trans* will generate circular DNA molecules (3C) (Dekker et al., 2002). Sequences interacting with a known gene (*IFN-β*) can be cloned by inverse PCR using gene-specific primers without any prior knowledge of their identities. HeLa cells were mock or virus infected for 4 hr, followed by formaldehyde crosslinking. The crosslinked chromatin was digested with EcoRI (flanking the *IFN-β* gene), followed by chromatin immunoprecipitation using a p65-specific antibody. The

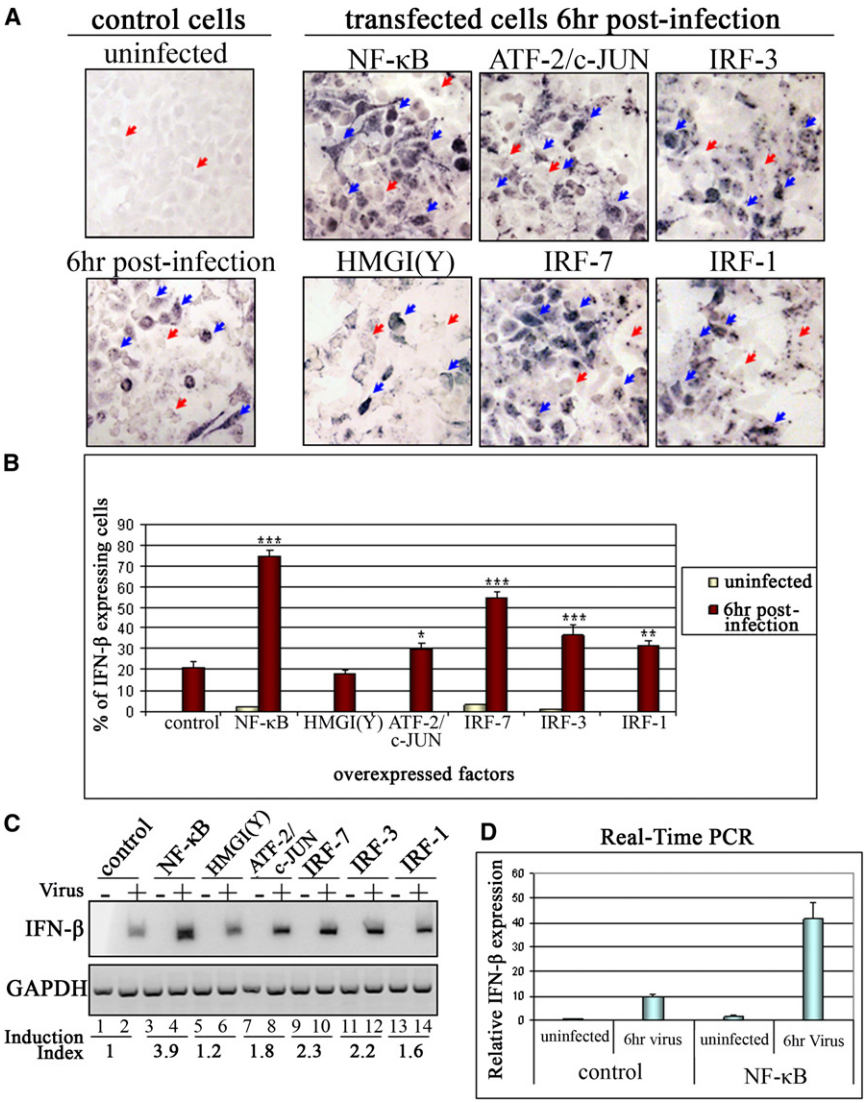

Figure 1. NF-κB Is the Most Limiting Factor Required for *IFN-β* Enhanceosome Assembly In Vivo

(A) HeLa cells were transfected with empty or expression vectors encoding each of the *IFN-β* gene activators. Six hours post-infection the cells were fixed and IFN-β expression in individual cells was detected by in situ hybridization using an antisense RNA *IFN-β* probe labeled with digoxygenin ribonucleotides followed by incubation with an anti-DIG antibody conjugated with alkaline phosphatase. The top left panel shows uninfected cells. The red and blue arrows indicate representative nonexpressing and expressing cells, respectively.

(B) Diagrammatic representation of the percentage (mean ± standard deviation [SD]) of cells expressing IFN-β from three independent in situ hybridization experiments performed as in (A). All cells for each category were scored blindly, and at least 300 cells were counted in each case. * denotes $p < 0.05$, ** denotes $p < 0.01$, and *** denotes $p < 0.001$.

(C) RT-PCR analysis illustrating IFN-β expression in HeLa cells transfected with the indicated *IFN-β* transcriptional regulators. The bottom part of the figure shows the induction index derived by quantitating three independent experiments.

(D) HeLa cells were transfected with the p65 expression vector along with a GFP-expressing plasmid followed by mock or virus infection. GFP-positive cells were isolated by cell sorting and the abundance of *IFN-β* mRNA was determined by real-time RT-PCR analysis (shown are mean values ± SD).

precipitated and digested chromatin was diluted and DNA ligase was added to covalently link DNA sequences that colocalize in the nucleus independent of their location. After removing the protein, nested PCR primers were used to detect interacting sequences. Using a pair of nested PCR primers (Figure 2A) we detected sequences from a wide range of sizes in the crosslinked chromatin (Figure 2B, lane 4) derived from virus-infected cells but not in any of the controls, including genomic DNA (Figure 2B, lane 1), EcoRI-cleaved but not ligated chromatin DNA (lane 2) derived from virus-infected cells, or EcoRI-cleaved and -ligated chromatin DNA derived from uninfected cells (lane 3). Subsequent sequence analysis of the 4C samples from virus-infected cells identified three unique sequences that appear to interact with *IFN-β* (Figures 2C and S1 available online). Remarkably, all three clones possess specialized Alu repeats, known as AluSX and AluY (Polak and Domany, 2006), which contain the putative NF-κB binding site GGGTTTCACC deviating from the consensus GGGRNYYCC in two nucleotides (underlined). Clones #14 and #9 contain two copies of the specialized NF-κB motif (Figure S1). Clone #21 resides on chromosome 4, #14 on chromosome 9, and #9 on chromosome 18. Of note, the *IFN-β* gene resides on chromosome 9 (9p21). Thus, #14 and *IFN-β* reside near the two ends of chromosome 9 in humans.

To examine whether the three identified loci interact with the *IFN-β* locus, we performed 3C assays using primers specific for *IFN-β* and for each of the clones. Figure 2D (lanes 1, 7, and 13) shows that in uninfected cells there is no detectable PCR product generated using primer pairs either from #21, or #14, or #9 and *IFN-β*. However, PCR products were detected when the chromatin DNA used was prepared from virus-infected cells (Figure 2D, lanes 2–4, 8–10, and 14–16). The products were detected as early as 2 hr after virus infection, peaked at 4 hr, and were decreased at 6 hr post-infection, indicating that these interactions occur primarily during enhanceosome assembly at the *IFN-β* locus. In each instance, the size of the PCR products was that predicted for the ligation of *IFN-β* with each of the clones and the identity of the products was confirmed by DNA sequence analysis (data not shown). Furthermore, the specificity of the interactions between the *IFN-β* locus and at least one of

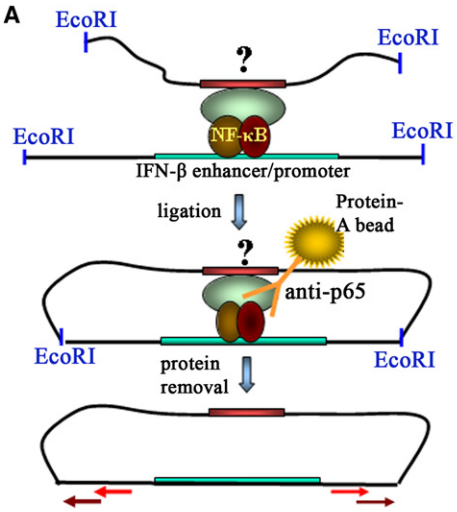

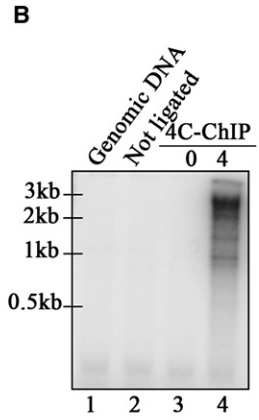

C

4C-ChIP clone number	Precise position	Nearby genes	Alu element
#21	4p13	19kb upstream of **RHOH** 20kb downstream of **N4BP2**	AluSX (GGGTTTCACC)
#14	9q33	10kb upsteram of **ABO** 15kb downstream of **LCN1**	AluY (GGGTTTCACC)
#9	18q21	12kb upstream of **LOXHD1**	AluSX (GGGTTTCACC)

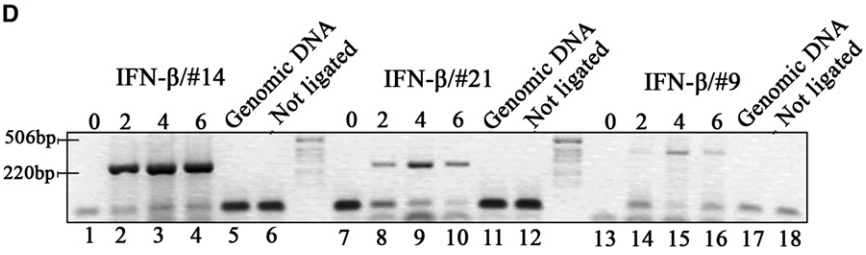

Figure 2. Identification of *IFN-β* Locus-Interacting Genomic Regions using 4C-ChIP

(A) Schematic representation of the 4C-ChIP assay. The EcoRI fragment bearing the *IFN-β* promoter is shown in green whereas EcoRI fragments bearing putative interacting loci are shown in red. The transcription factor NF-κB is shown bound on the *IFN-β* enhancer. The red arrows indicate nested primers designed near the EcoRI sites flanking the *IFN-β* locus.

(B) Shown is an agarose gel depicting nested inverse polymerase chain reactions of 4C-ChIP samples. After amplification only crosslinked, digested, and ligated chromatin DNA derived from virus-infected cells generated amplified sequences of different sizes.

(C) Short description of 4C-ChIP clones.

(D) Agarose gel electrophoresis of the PCR products using nested primers specific to the *IFN-β* locus together with primers specific for the 4C-ChIP clones #14, #21, and #9. PCR was performed on EcoRI-digested chromatin derived from HeLa cells mock- or virus-infected for 2, 4, and 6 hr. Genomic DNA and crosslinked digested but not ligated chromatin derived from 4 hr infected cells were used as controls. Size markers were loaded between lanes 6 and 7, 12 and 13.

the clones (#21) was verified in 4C-ChIP experiments using inverse PCR-nested primers from the genomic locus of #21. In this experiment we cloned the *IFN-β* locus three times, underscoring the strength and the specificity of these interactions (data not shown).

To further validate the 4C data and to demonstrate the physical colocalization of IFN-β with clones #21, #9, and #14, we performed three-dimensional DNA fluorescence in situ hybridization (FISH) analysis using HeLa cells that were either mock or virus infected for 4 hr. Figure 3A shows that the *IFN-β* probe detects six or seven *IFN-β* genes, whereas probes for #21, #9, and #14 detect three, three, and six or seven loci in HeLa cells, respectively. This is due to the fact that HeLa cells are polyploid. In mock-infected cells we detected no evidence of colocalization between *IFN-β* and any of the clones (Figure 3A, left column). Remarkably, in some virus-infected cells, one allele of *IFN-β* is specifically colocalized with one allele of #21, or #14, or #9 (Figure 3, right column). FISH experiments using a BAC clone containing different AluSX repeats fail to detect colocalization with the *IFN-β* locus before or after virus infection (not shown). These FISH experiments confirmed our results obtained using the 3C technique (Figure 2). FISH experiments performed on nuclei from virus-infected cells for different amounts of time indicated that these interactions are transient since they appear 2 hr post-infection, peak at 4 hr, and decline significantly at 8 hr post-infection (Figure 3B), a result consistent with the 3C analysis of Figure 2D. Thus, interchromosomal associations between the *IFN-β* locus and these loci occur at maximal frequencies before initiation of transcription and during enhanceosome assembly (2–6 hr), and they are significantly reduced at the time of initiation and propagation of transcription (6–8 hr).

In control experiments, FISH was performed with the *IL-8* gene (a known NF-κB target virus-inducible gene) and clones #21, #14, and #9 in mock- or virus-infected cells. No specific colocalization was detected between these loci and the *IL-8* gene, nor between the *IFN-β* and *IL-8* genes (data not shown). By contrast, the 4C clone #21 (#14 and #9 not shown) was colocalized with the *IκBα* gene (another NF-κB target) (Figure S2). The interaction between *IκBα* and our 4C clones prompted us to examine whether the *IFN-β* and *IκBα* genes are colocalized after virus infection. As seen in Figure S2, 11% of virus-infected cells show colocalization between the *IFN-β* and *IκBα* genes. Thus, the *IFN-β* and *IκBα* genes, which are activated by NF-κB, colocalize after virus infection. These colocalizations appear to be gene specific since not all NF-κB-regulated genes colocalize either with the 4C clones or between them.

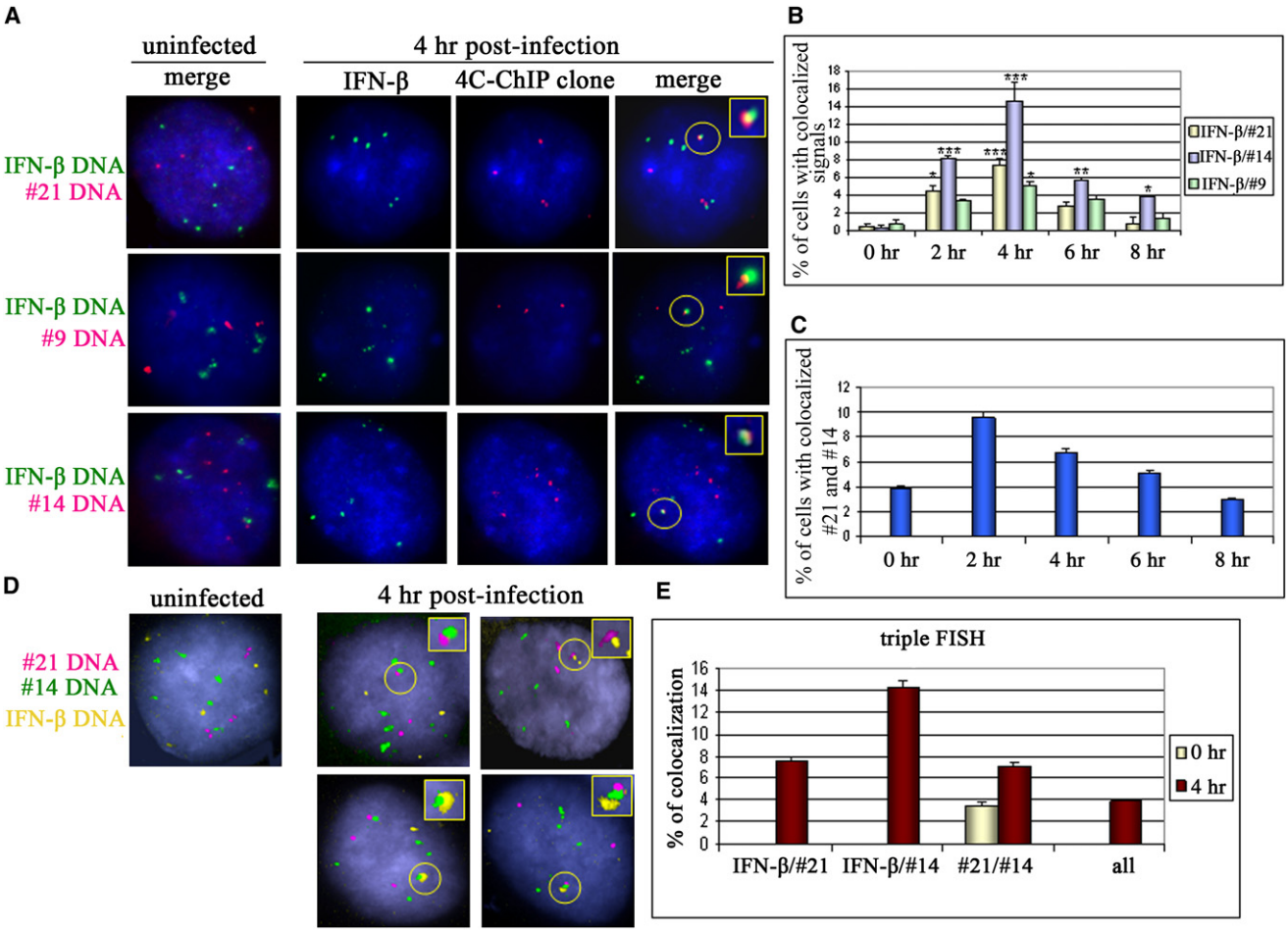

Figure 3. DNA FISH Reveals the Colocalization of the *IFN-β* Locus and the 4C-ChIP Clones following Virus Infection

(A) A digoxygenin-labeled DNA probe was used to detect the *IFN-β* locus and was visualized with FITC-conjugated anti-DIG antibody (green). A biotin-labeled DNA probe was used to detect the 4C-ChIP clones, as indicated in the figure, and was visualized with Alexa 568-conjugated streptavidin (red). The circle includes the colocalized alleles observed only in virus-infected cells. A magnification of the area of colocalization is shown at the top right.

(B) Diagrammatic representation of the percentage (mean ± SD) of cells with colocalization between *IFN-β* and each of the 4C-ChIP clones during the time course of virus infection. All cells were scored blindly and slides were prepared from three different experiments. Scores were derived from 250 to 486 cells for each category. * denotes $p < 0.05$, ** denotes $p < 0.01$, and *** denotes $p < 0.001$.

(C) Diagrammatic representation of DNA FISH experiments showing the percentage (mean ± SD) of cells with colocalized signals of #21 and #14 in the time course of virus infection. Of note, relatively high frequency of colocalization is observed in uninfected cells.

(D) Triple DNA FISH experiment revealed the simultaneous colocalization of *IFN-β* with #21 and #14 upon virus infection. The *IFN-β* locus was detected with far red (yellow).

(E) Diagrammatic representation of triple DNA FISH experiments showing the percentage (mean ± SD) of cells with colocalized signals of each combination of the indicated genomic loci.

To test whether the 4C isolated genomic loci colocalize before or after virus infection, we carried out FISH experiments using probes for each 4C clone. The results showed a markedly high frequency of colocalization between 4C clones #14 and #21 even before virus infection (Figure 3C). These interactions are specific since the *IFN-β* gene located on the same chromosome as #14 does not colocalize with any of these clones before virus infection. The interchromosomal interactions are further increased upon virus infection (Figure 3C). Remarkably, triple FISH experiments revealed the simultaneous interaction of *IFN-β* with these 4C loci, albeit in a lower percentage of cells (Figures 3D and 3E). These results showed that the widely separated 4C clones colocalize before virus infection and interact together with the *IFN-β* gene after virus infection.

4C Clones Colocalize with Monoallelically Expressed *IFN-β* RNA

We have shown that one *IFN-β* allele interacts with one allele from each of the 4C clones only in response to virus infection (Figure 3). At the peak of interaction (Figure 3B), the total percentage of *IFN-β* interacting alleles in the cell population is 27%, a number that is similar to the percentage of cells expressing IFN-β following virus infection (Figure 1). Therefore, we asked whether these interchromosomal interactions correlate with

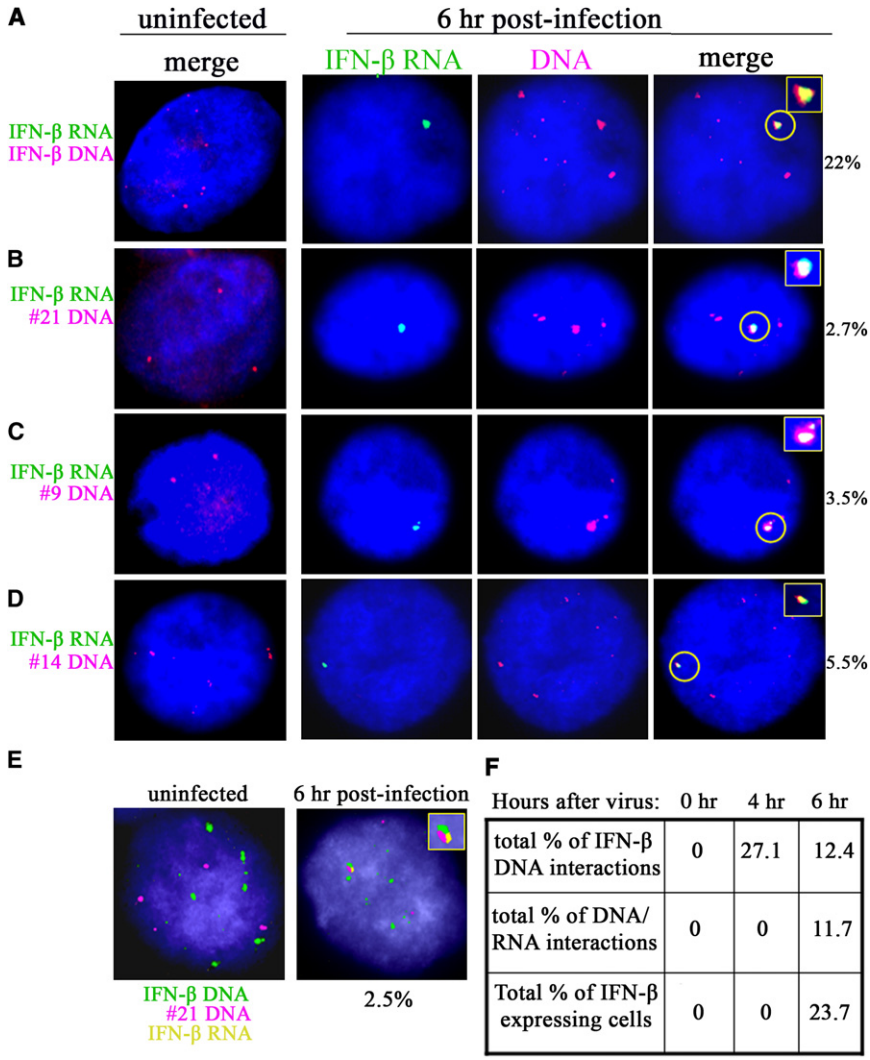

Figure 4. RNA and DNA FISH on Virus-Infected Cells Reveal Colocalization of the 4C-ChIP Clones with the Transcriptionally Active *IFN-β* Allele

(A) Combined RNA and DNA FISH on nuclei from mock- and virus-infected for 6 hr HeLa cells. DIG-labeled nick-translated *IFN-β* probe was used for the detection of the *IFN-β* nuclear transcripts. The signal was visualized with FITC-conjugated anti-DIG antibody (green). A biotin-labeled DNA probe was used for the detection of the *IFN-β* locus and was visualized with Alexa 568-conjugated streptavidin (red). The nuclei were counterstained with DAPI (blue). RNA FISH detects the virus-inducible single transcriptionally active *IFN-β* allele, whereas DNA FISH detects all 6 *IFN-β* alleles in HeLa cells. The percentage of expressing cells is shown on the right.

(B) RNA FISH to detect *IFN-β* nuclear RNA (green) combined with DNA FISH detecting the #21 locus (red). The transcriptionally active *IFN-β* allele colocalizes with a single #21 allele at a frequency indicated at the right.

(C) RNA FISH to detect *IFN-β* nuclear RNA (green) combined with DNA FISH detecting the #9 locus (red). The transcriptionally active *IFN-β* allele colocalizes with a single #9 allele at a frequency indicated at the right.

(D) RNA FISH to detect IFN-β nuclear RNA (green) combined with DNA FISH detecting the #14 locus (red). The transcriptionally active *IFN-β* allele colocalizes with a single #14 allele at a frequency indicated at the right.

(E) Triple RNA/DNA FISH experiment revealed the simultaneous colocalization of the *IFN-β* gene (green) with #21 (red) and *IFN-β* mRNA (yellow) upon virus infection.

(F) Frequency of colocalization of *IFN-β* with the 4C clones and its correlation with monoallelic stochastic *IFN-β* expression.

IFN-β RNA production. We combined DNA FISH with RNA FISH to determine whether the 4C clones colocalize with the transcribed *IFN-β* gene following virus infection. Figure 4A shows that only one IFN-β allele is transcribed at 6 hr following virus infection. Remarkably, this allele colocalizes with a single allele from the 4C clones (Figures 4B–4D) with frequencies similar to those described in Figure 3B for the 6 hr time point. The triple RNA/DNA FISH experiment of Figure 4E shows that the single *IFN-β* allele interacting with the 4C clone #21 is the one expressing *IFN-β* mRNA. As a control we showed that the *IFN-β* RNA is not detected in uninfected cells and that the *IFN-β* RNA signal is lost when virus-infected cells are treated with RNase A (data not shown). Taken together, these results suggest that interchromosomal associations occurring between single alleles from the 4C clones and *IFN-β* in a cell population correlate with monoallelic *IFN-β* transcription. The total percentage of cells showing maximal monoallelic interchromosomal interactions at 4 hr post-infection (27.1%, Figure 4F) correlates to the total percentage of cells expressing the *IFN-β* gene from a single allele at 6 hr (22%, Figure 4A). These experiments suggest that the *IFN-β* RNA is transcribed from a single *IFN-β* allele interacting with a single allele from any of the 4C isolated loci.

Since the experiments described above have been carried out in HeLa cells that are polyploid, we repeated the DNA, DNA-RNA FISH, and the triple FISH experiments in diploid human epithelial cells (HCT-116) and obtained qualitatively similar results (Figure S3), thus indicating the biological significance of our observations.

IFN-β Gene Transcription Switches from Monoallelic to Multiallelic in Response to IFN-β Cytokine Signaling

The experiments of Figure 4 were performed using cells infected with virus for 6 hr. This is the time point at which *IFN-β* transcription begins. However, at this time point there is a decreased interaction between *IFN-β* and the 4C clones, and this interaction is lost at the peak of *IFN-β* transcription (Figure 3). Since there are no interchromosomal interactions at later time points (not shown) we can't further correlate *IFN-β* RNA expression with interaction with the 4C clones. However, when we repeated the DNA-RNA FISH using *IFN-β* probes and cells infected with

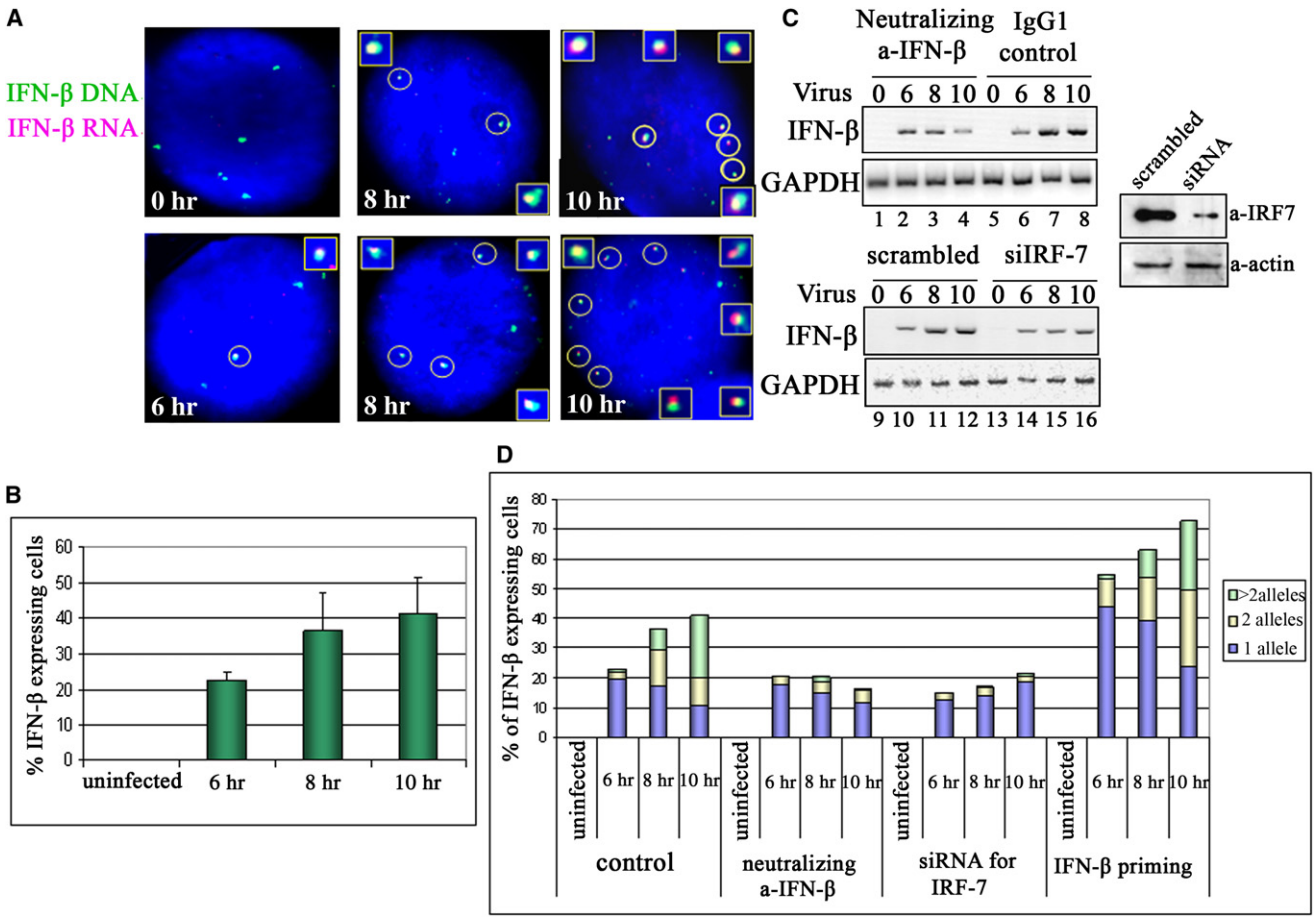

Figure 5. *IFN-β* Gene Transcription Switch from Monoallelic to Multiallelic during the Time Course of Virus Infection Requires IRF-7

(A) Combined RNA and DNA FISH on nuclei from mock- and virus-infected HeLa cells for 6, 8, and 10 hr. Biotin-labeled nick-translated *IFN-β* probe was used for the detection of the *IFN-β* nuclear transcripts. The signal was visualized with Alexa 568-conjugated streptavidin (red). A DIG-labeled DNA probe was used for the detection of the *IFN-β* locus and was visualized with FITC-conjugated anti-DIG antibody (green). The nuclei were counterstained with DAPI (blue). RNA FISH detects a single transcriptionally active *IFN-β* allele at 6 hr post-infection and additional *IFN-β*-expressing alleles at later time points.

(B) Diagrammatic representation of the percentage (mean ± SD) of cells expressing IFN-β from three independent in situ hybridization experiments performed as in Figure 1 except that the cells were infected with virus for 6, 8, or 10 hr. All cells for each category were scored blindly and at least 220 cells were counted in each case.

(C) HeLa cells were mock- or virus-infected for 6, 8, or 10 hr in the presence of IFN-β neutralizing antibodies or IgG1 as a control (lanes 1–8). RNA was isolated and the abundance of the *IFN-β* transcripts was determined by RT-PCR analysis. In the bottom panel (lanes 9–16) the cells were treated with scrambled siRNA or siRNA specific for IRF-7 for 62 hr before virus infection and RT-PCR analysis. The efficiency of the siRNA knockdown was tested by western blot (shown on the right of the figure) using extracts prepared from virus-infected cells.

(D) Diagrammatic representation of the percentage of cells and the number of *IFN-β*-expressing alleles per cell from two independent RNA/DNA FISH experiments performed as in Figure 4 except that the cells were treated as in (C). All cells for each category were scored blindly and at least 130 cells were counted in each case. In each column the relative percentage of cells expressing 1, 2, or more *IFN-β* alleles is indicated with different colors.

Sendai virus for longer times we found that gradually the remaining *IFN-β* alleles begin to express *IFN-β* RNA (Figure 5A), a result consistent with the gradual decrease of intrinsic noise of *IFN-β* expression reported recently (Hu et al., 2007). The in situ hybridization experiment of Figure 5B shows that the percentage of cells expressing IFN-β is nearly doubled at 10 hr post virus infection as opposed to the percentage of expressing cells at 6 hr post-infection. In summary, *IFN-β* transcription begins from a single allele interacting with the 4C clones in 20% of the cells but at later time points the remaining *IFN-β* alleles, not interacting with the 4C clones, begin to express IFN-β in the same and in other cells.

To test whether the IFN-β protein produced early in virus infection from a single allele is critical for the subsequent multiallelic expression (positive feedback) of the same and other cells we added neutralizing IFN-β antibodies in the culture. Figure 5C shows that the neutralizing antibodies dramatically decreased IFN-β expression at 8 and 10 hr post-infection, but they did not affect the early monoallelic activation of the gene (compare lanes 1–4 with 5–8). To determine whether the effect of the IFN-β protein on *IFN-β* gene expression is mediated through IRF-7, which is an IFN-β-inducible factor (Sato et al., 2000), we treated the cells with an IRF-7-specific siRNA. As seen in Figure 5C (lanes 9–16), IRF-7 is critical for maximal *IFN-β* transcription especially

at the later time points, and it has a small effect at the early phase of induction, a result consistent with the late arrival of IRF-7 on the *IFN-β* enhancer (Munshi et al., 2001).

To correlate the IFN-β protein effect on *IFN-β* gene transcription with the switch from mono- to multiallelic expression we carried out DNA and RNA FISH experiments to determine the number of *IFN-β* alleles expressing the *IFN-β* gene. Figure 5D shows that 22% of the cells infected with Sendai virus for 6 hr express IFN-β, and of these the majority (19% of total cells) transcribe the *IFN-β* gene from a single allele. However, at 8 hr post-infection there is a parallel decrease of monoallelic expressing cells and an increase of cells expressing IFN-β from two or more alleles. This switch is more dramatic at 10 hr post-infection when the majority of the expressing cells transcribe the *IFN-β* gene from two or more alleles. Treatment of the cell culture with neutralizing IFN-β antibodies affected monoallelic expression only slightly, but it dramatically reduced both the total number of cells expressing IFN-β at later time points and the switch from mono to multiallelic IFN-β expression. A similar result was obtained when the cells were treated with the IRF-7-specific siRNA (Figure 5D). These experiments demonstrate that the IFN-β protein secreted early on at virus infection is produced from cells transcribing a single *IFN-β* gene allele and acts on the same and on other cells to induce *IFN-β* gene transcription on all alleles. A prediction from these experiments is that treatment of the cells with IFN-β before virus infection (IFN-β priming) would increase the number of expressing cells and the number of expressing alleles. Indeed, Figure 5D shows that IFN-β priming doubles the number of expressing cells and increases the number of alleles expressing the *IFN-β* gene, without affecting the frequency of interchromosomal interactions (data not shown). Thus, the IFN-β signaling-dependent effect is mediated by the IRF-7 transcription factor.

4C Isolated Loci Increase the Probability for IFN-β Expression

If the early monoallelic expression of the *IFN-β* gene in a small cell population depends on the stochastic nature of the interchromosomal interactions between the *IFN-β* gene and the 4C isolated loci, then increasing the copy number of any of the 4C clones might increase the number of the cells expressing IFN-β predominantly from a single allele. To test this idea we transfected HeLa cells with a bluescript vector harboring the #21, #9, and #14 clones, followed by virus infection. Figure 6A shows that transfection of any of the 4C plasmids increased the levels of *IFN-β* and *IκBα* gene expression after virus infection from 3- to 5-fold. As a control, we showed that the levels of *IL-8* expression were not affected, a result consistent with the fact that the *IL-8* gene does not interact with the 4C clones. Importantly, 3C experiments confirmed that the transfected 4C plasmids interact specifically with the endogenous *IFN-β* locus in a virus-infection-dependent manner (data not shown). Figure 6B shows that at least part of the *IFN-β* RNA increase is due to an increase in the number of cells expressing *IFN-β* RNA. Transfection of a construct derived from #21 harboring just the AluSX repeat also led to an increase in the number of cells expressing IFN-β but to a lesser extent than the full-length #21. Remarkably, transfection of a #21 construct harboring a precise deletion of the nonconsensus NF-κB site marginally only affected *IFN-β* RNA levels or the number of cells expressing the gene (Figures 6A and 6B). Thus, the NF-κB site of the 4C clones plays a critical role in determining the probability of IFN-β expression in each cell. One possibility could be that NF-κB associates first with the 4C clones and then is transferred to the *IFN-β* locus via interchromosomal interactions. Indeed, chromatin immunoprecipitation experiments revealed that NF-κB binds to the 4C clones earlier after virus infection than it binds to the *IFN-β* promoter (Figure 6C). More specifically, at 1 hr after virus infection NF-κB associates with the 4C clones, whereas at the same time binding at the *IFN-β* promoter is not detected (Figure 6C, lane 2). Maximal NF-κB binding to DNA corresponding to the 4C clones (lane 5) correlates with the maximal frequency of interchromosomal associations with the *IFN-β* locus (4 hr), and this correlates also with maximal recruitment of NF-κB to the *IFN-β* promoter.

To determine the ratio of mono- to multiallelic *IFN-β* gene expression after transfection of the 4C clones we carried out DNA-RNA FISH experiments on virus-infected HeLa cells. Figure 6D shows that transfection of the 4C clone #21 increased the probability of expression without affecting significantly the ratio of mono to multiallelic expression at 6 hr post-infection. The specificity of this phenomenon was underscored by the inability of the mutant 4C #21 (ΔNF-κB) to increase the number of expressing cells. A qualitatively similar result was obtained when we transfected NF-κB or IRF-7 expressing vectors (Figure 6D), an observation consistent with the fact that these factors are limiting in the cells. However, when both factors were expressed at high levels within the cells, *IFN-β* transcription began simultaneously at many more cells and at more than one allele per cell and only in virus-infected cells, further underscoring the requirement for assembly of a complete enhanceosome.

DISCUSSION

In this study we present evidence for a model to explain how virus infection induces the stochastic expression of the *IFN-β* gene (Figure 7). According to this model, the choice of the allele to be expressed depends on stochastic interchromosomal associations between the *IFN-β* gene and at least one of the three identified distinct genomic loci that could mediate binding of the transcription factor NF-κB to the *IFN-β* enhancer. Then, NF-κB nucleates enhanceosome assembly, a prerequisite for chromatin remodeling, and activation of transcription from this allele. The secreted IFN-β protein acts in a paracrine and autocrine manner to signal the presence of virus infection by inducing the expression of hundreds of genes that together establish the "antiviral state" (Stetson and Medzhitov, 2006). One of the genes activated by IFN-β is *IRF-7*, a transcription factor that associates with the IFN-β enhanceosome late in infection. The increased intracellular levels of IRF-7 trigger enhanceosome assembly in additional cells and on multiple *IFN-β* alleles in each cell, thus amplifying the production of IFN-β. This second phase of *IFN-β* transcription occurs independently of interchromosomal associations (Figure 7).

The precise organization of the *IFN-β* enhanceosome is required for optimal cooperative occupancy in response to viral

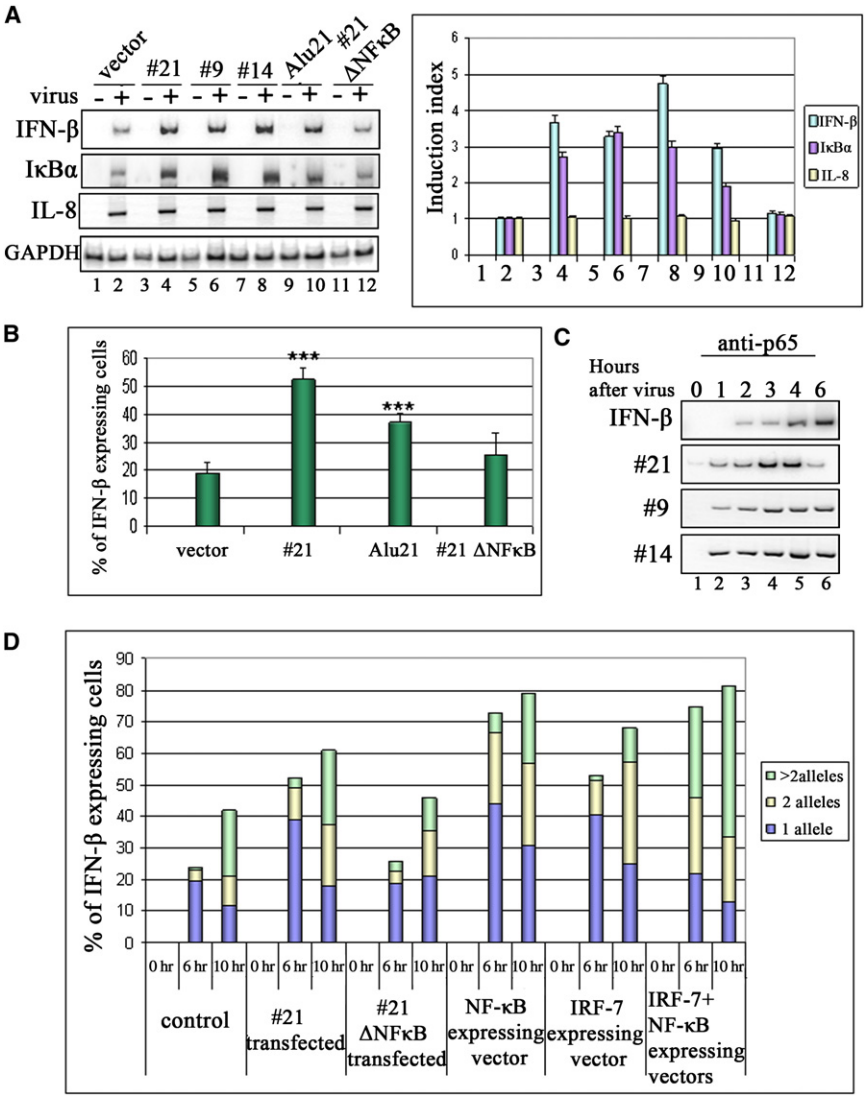

Figure 6. 4C-ChIP Clones Increase the Probability of Stochastic *IFN-β* Gene Expression

(A) HeLa cells were transfected with bluescript–based constructs bearing the 4C-ChIP clones #21, #9, and #14, a derivative of #21 containing only the Alu SX (Alu21) repeat or, a mutant of #21 lacking the NF-κB site (#21ΔNF-κB). The cells were infected with virus for 6 hr and the isolated RNA was used as a template for RT-PCR analysis using primers specific for *IFN-β*, *IκBα*, and *IL-8* genes. The radioactive bands were quantitated using phosphorImager and the data from four independent experiments were plotted and are shown at the right panel of the figure (shown are mean values ± SD).

(B) Diagrammatic representation of the percentage (mean ± SD) of cells expressing IFN-β from three independent in situ hybridization experiments performed as in Figure 1 except that the cells were transfected with the indicated bluescript-based constructs. All cells for each category were scored blindly and at least 300 cells were counted in each case. *** denotes $p < 0.001$.

(C) Crosslinked chromatin prepared from mock- or virus-infected HeLa cells for the indicated amount of time was immunoprecipitated with the p65-specific antibody. The precipitated *IFN-β* promoter and #21, #14, and #9 loci were detected by PCR using ^{32}P-dCTP in the reaction.

(D) Diagrammatic representation of the percentage of cells and the number of *IFN-β*-expressing alleles per cell from two independent RNA/DNA FISH experiments performed as in Figure 4 except that the cells were transfected with the indicated plasmids. All cells for each category were scored blindly and at least 180 cells were counted in each case. In each column the relative percentage of cells expressing 1, 2, or more *IFN-β* alleles is indicated with different colors.

infection in vivo, and it has been suggested that such an organization may reflect regulation by limiting concentrations of one or more critical activators (Papatsenko and Levine, 2007). The low concentration of NF-κB and IRF-7 explains the ordinary requirement for cooperativity in enhanceosome assembly and sets the stage for combinatorial control of transcription. On the other hand this poses a problem, that is, how to target a low abundance factor like NF-κB to the correct gene for nucleating enhanceosome assembly in a nucleus containing millions of putative NF-κB binding sites.

We have identified three genomic loci that interact separately or in combinations with a single allele of *IFN-β* (Figures 7A and 7B) in response to virus infection. Two of these loci map in different chromosomes than the *IFN-β* gene, whereas the third is on the same chromosome but on the other arm. We have been unable to clone additional loci interacting with *IFN-β* with the 4C-ChIP approach, presumably due to the high false negative rate of the approach. However, this does not exclude the possibility that the *IFN-β* locus can interact with additional loci with lower frequencies and affinities. The physical association of these distant DNA sequences with the IFN-β gene occurs during the time of enhanceosome assembly and before initiation of transcription. Thus, it is possible that these interchromosomal associations play a role in enhanceosome assembly by facilitating (delivering) NF-κB binding to the *IFN-β* promoter. The following observations are consistent with this model. First, chromatin immunoprecipitation experiments revealed that NF-κB binds to the 4C clones before binding to the *IFN-β* promoter. Second, the interchromosomal interactions are NF-κB dependent as revealed by transfecting the cells with a dominant-negative form of IκBα (ΔN-IκBα), leading to a dramatic decrease of both virus-inducible interchromosomal interactions and IFN-β expression (Figure S4). The third observation supporting a role of the 4C clones in delivering NF-κB is the experiment shown in Figure S5. We transfected p65 followed by virus infection and found a significant decrease in the frequency of interchromosomal interactions, thus suggesting that these associations take place only when the concentration of NF-κB within the cells is at

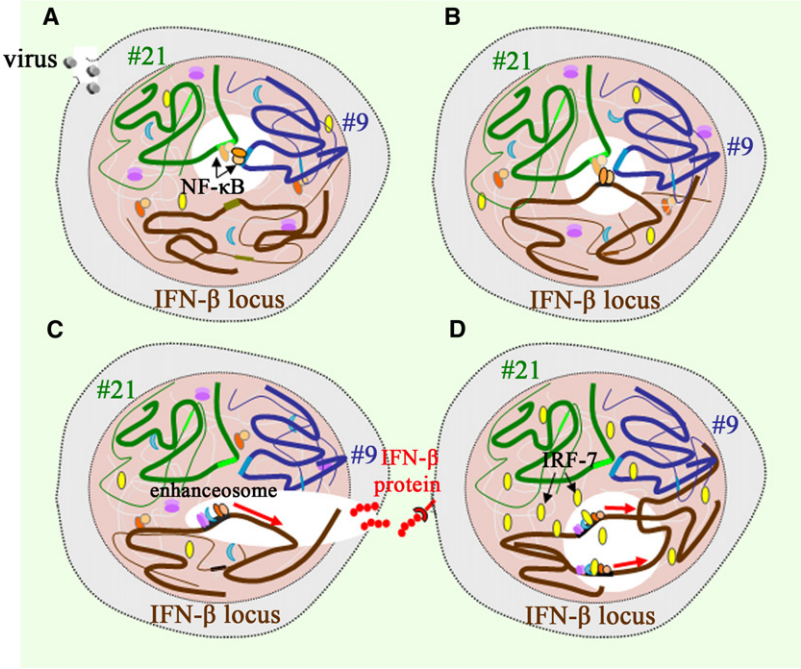

Figure 7. A Model Depicting Stochastic Activation of *IFN-β* Gene Transcription

(A) Virus infection induces the nuclear localization of NF-κB, which binds first to a site in the nucleus where single alleles of the 4C-ChIP loci are in physical proximity.

(B) Next, one allele of *IFN-β* interacts with the 4C-ChIP loci and NF-κB is transferred to the *IFN-β* enhancer. This stochastic reactions takes place in ~20% of the cells and involves a single *IFN-β* allele.

(C) NF-κB nucleates enhanceosome assembly on this allele leading to monoallelic activation of transcription.

(D) The secreted IFN-β protein acts on the same and on other not initially expressing cells to induce high-level transcription of IRF-7. The IRF-7 protein accumulates at high levels and binds to the *IFN-β* enhancer stimulating enhanceosome assembly on more than one allele. This leads to multiallelic expression and amplification of the virus infection-induced signal.

physiological low levels. Furthermore, the observation that these loci are in physical proximity before the entrance of NF-κB into the nucleus suggests that it is the *IFN-β* gene that is recruited to this site to "receive" NF-κB. When the levels of NF-κB are increased by transfection, the factor can bind to the *IFN-β* promoter independently of interchromosomal associations. We propose the existence of an NF-κB "receptor" center consisting of the 4C loci that can immediately receive NF-κB and distribute the factor to the promoters of selected genes via interchromosomal associations. We can imagine that the NF-κB receptor center is localized in specialized nuclear regions to which the incoming NF-κB can have instant access. Support for such a model comes from the fact that the affinity of NF-κB for these sites is 2–3 times lower than that for the *IFN-β* gene (our unpublished data), thus implying that its preference for the receptor center could be due to a combination of factors such as the local nuclear architecture, DNA-induced allostery, and/or other proteins localized in this microenvironment. We do not know the mechanisms assuring the specificity of these interchromosomal associations since not all NF-κB-regulated genes (e.g., *IL-8*) are recruited to the NF-κB center. It is possible that additional factors bound to the 4C clones and/or to the promoters of the recruited genes determine the specificity of the interactions by exposing complementary surfaces. A prediction derived from our model is that conversion of the low-affinity specialized NF-κB site present in the 4C clones to a consensus high-affinity site would preclude the delivery of NF-κB to the *IFN-β* enhancer, resulting in a decrease in transcription. Figure S6 shows that the 4C clones bearing a consensus high-affinity NF-κB site taken from the MHC class I are not only incapable of facilitating *IFN-β* expression but also decrease *IFN-β* transcription, presumably by serving as competitors. Additional support for our model is provided by the observation that all 4C clones contain specialized Alu repeats, and that the Alu NF-κB site is an integral functional component of the repeats required for the stochastic IFN-β expression. Previous studies have shown that Alu repeats are euchromatic and contain several functional transcription factor-binding sites and may play a role in regulation of biological processes (Polak and Domany, 2006). We can imagine that Alu repeats interspersed in the genome may function as "marks" to properly align interacting chromosomal domains during the execution of several nuclear processes.

The model we propose stipulates that the stochastic activation of only one allele is dependent on the limited concentration of NF-κB, and it could explain the monoallelic and stochastic expression of many other cytokines regulated by NF-κB. Furthermore, the stochastic oscillation of NF-κB in individual cells further underscores the requirement for a promoter-targeting mechanism to ensure the proper activation of immune genes (Nelson et al., 2004). The formation of a complex between *IFN-β* and the 4C clones is a rapid signal-dependent process that occurs within 2 hr of virus infection, thus differing from other types of interchromosomal interactions described in olfactory receptor expression (Lomvardas et al., 2006), T cell differentiation (Spilianakis et al., 2005), HoxB1-dependent ES differentiation (Wurtele and Chartrand, 2006), imprinting (Ling et al., 2006; Zhao et al., 2006), erythroid gene expression (Osborne et al., 2004), X chromosome inactivation (Bacher et al., 2006; Xu et al., 2006), etc., which are established during long-lasting cell differentiation pathways. Furthermore, the interchromosomal interactions described here occur between a known gene and intergenic loci with previously unknown function.

The monoallelically produced and secreted IFN-β protein activates among others the *IFN-β* gene activator IRF-7. Before virus infection, IRF-7 is expressed at very low amounts and has a very short half-life, and, like IRF-3, virus infection induces serine phosphorylation allowing IRF-7's dimerization and nuclear translocation (Honda et al., 2006). This observation is consistent with our siRNA experiments, which revealed a small contribution of IRF-7 in the initial monoallelic expression of *IFN-β* but

underscored its role in late multiallelic *IFN-β* transcription. We believe that the high levels of IRF-7 production in response to IFN-β signaling drive enhanceosome assembly in more cells and in more than one allele per cell (Figure 7D). As predicted, IRF-7 overexpression experiments and IFN priming increased the number of expressing cells and alleles. In other words, the "pioneer" factor that nucleates enhaceosome assembly in the second phase appears to be IRF-7 as opposed to NF-κB in the first phase.

In summary, we present evidence that the limiting factor NF-κB is delivered to a single *IFN-β* allele via stochastic interchromosomal associations, and this nucleates enhanceosome assembly by "recruiting" the remaining factors via DNA-induced conformational changes and protein-protein interactions leading to transcriptional activation. Next, the remaining *IFN-β* alleles are activated through the IRF-7-driven assembly of enhanceosomes and independently of interchromosomal associations (Figure 7). Consistent with this idea is our observation that overexpression of both p65 and IRF-7 leads to the simultaneous expression of *IFN-β* from multiple alleles even at the early phase of expression. Thus, our experiments provided a mechanistic model of how the *IFN-β* enhancer integrates inputs received from virus infection and signal amplification derived from the positive IFN feedback loop.

EXPERIMENTAL PROCEDURES

Tissue Culture and Cell Transfection and In Situ Hybridization

HeLa CCL-2 (ATCC) and HCT-116 cells were cultured in DMEM supplemented with 10% FBS and 1% PENSTREP at 37°C. All transfections were performed with lipofectamine 2000 (Invitrogen) according to the manufacturer's instructions. Cells transfected with siRNA for IRF-7 (sc-38011, SantaCruz Biotechnology) were grown for 62 hr before virus infection. In situ hybridizations were performed as described previously (Senger et al., 2000).

3C and 4C-ChIP

The 3C analysis was performed as described previously (Dekker et al., 2002). The detailed procedure is described in the Supplemental Data. For the 4C-ChIP, the cells were treated as in the 3C. After EcoRI restriction, the cleaved chromatin was dialyzed in a buffer containing 5% glycerol, 10 mM Tris-HCl (pH 8), 1 mM EDTA, and 0.5 mM EGTA overnight (O/N) at 4°C. Fifty micrograms of the chromatin was used for immunoprecipitation with the anti-p65 antibody as previously described (Agelopoulos and Thanos, 2006). After the final wash with TE, a small sample of the beads was removed in order to check the ChIP efficiency. The bead-bound fragments were ligated O/N, at 16°C with 100 U of ligase in 1 ml final volume, followed by addition of ligase and ATP and incubation at room temperature (RT) for 3 hr. The immunoprecipitated and ligated DNA was isolated and used as template for inverse-nested PCR (Figure S5). The products were analyzed and isolated from a 1.5% agarose gel and cloned in pGEM Teasy vector (Promega), and the positive clones were analyzed by DNA sequencing.

DNA and DNA/RNA FISH

The DNA FISH analysis was performed as described in the Supplemental Data. The BAC probes used were obtained from CHORI BACPAC libraries. Specifically we used the following: RPCI-11.113D19 for the *IFN-β* locus, RPCI-11.447E20 for the *IL-8* locus, RPCI-11.395I6 for #21, RPCI-11.81F13 for *IκBα*, RPCI-11.418K9 for #9, RPCI-11.430N14 for #14, and CTB-BRI 64I22 for the AluSx control clone. For the DNA/RNA FISH, the cells were attached on glass slides, were washed with ice-cold PBS, and incubated for 10 min in cytoskeleton buffer containing 100 mM NaCl, 300 mM sucrose, 3 mM $MgCl_2$, 10 mM Pipes, 0.1% Triton X-100, and 20 mM vanadyl-ribonucleoside, and were then fixed for 15 min at RT in a solution containing 4% PFA in PBS with 5% acetic acid. The slides were then incubated overnight in 70% ethanol at 4°C. The next day the permeabilized cells were incubated in 50% formamide-2× SSC at 70°C for 3 min and dried in ethanol series. The probes after heat denaturation were applied directly on the dried cells and incubated O/N at 37°C. The slides were washed two times for 10 min in a solution of 50% formamide in 2× SSC at 37°C. After 30 min of blocking at RT the signal was detected with incubation of anti-DIG/ Fluorescein antibody or streptavidin/ Alexa 568 in a solution containing 0.1 M Tris-HCl (pH 8), 0.15 M NaCl, 1× blocking reagent (Roche), and 20 mM vanadyl-ribonucleoside complex. The antibody was crosslinked in 4% PFA in PBS for 10 min at RT. Then DNA FISH was performed using the NaOH denaturation protocol described above.

SUPPLEMENTAL DATA

Supplemental Data include Supplemental Experimental Procedures and seven figures and can be found with this article online at http://www.cell.com/cgi/content/full/134/1/85/DC1/.

ACKNOWLEDGMENTS

We thank Sarantis Gagos for help with the DNA FISH and Marios Agelopoulos for advice with the ChIP experiments. We also thank Tom Maniatis, Richard Mann, Stavros Lomvardas, Ethan Ford, Mat Lavigne, George Panayotou, and George Mosialos for critical reading of the manuscript. This work was supported from grants to D.T. from the Greek Secreteriat for Research and Technology (03PENED-422), March of Dimes, Association for International Cancer Research, and EU (FP6 Transfog). E.A. was partially supported from the Greek National Foundation of Scholarships.

Received: December 21, 2007
Revised: March 18, 2008
Accepted: May 3, 2008
Published: July 10, 2008

REFERENCES

Agalioti, T., Lomvardas, S., Parekh, B., Yie, J., Maniatis, T., and Thanos, D. (2000). Ordered recruitment of chromatin modifying and general transcription factors to the IFN-beta promoter. Cell *103*, 667–678.

Agelopoulos, M., and Thanos, D. (2006). Epigenetic determination of a cell-specific gene expression program by ATF-2 and the histone variant macroH2A. EMBO J. *25*, 4843–4853.

Bacher, C.P., Guggiari, M., Brors, B., Augui, S., Clerc, P., Avner, P., Eils, R., and Heard, E. (2006). Transient colocalization of X-inactivation centres accompanies the initiation of X inactivation. Nat. Cell Biol. *8*, 293–299.

Calado, D.P., Paixao, T., Holmberg, D., and Haury, M. (2006). Stochastic monoallelic expression of IL-10 in T cells. J. Immunol. *177*, 5358–5364.

Dekker, J., Rippe, K., Dekker, M., and Kleckner, N. (2002). Capturing chromosome conformation. Science *295*, 1306–1311.

de Laat, W., and Grosveld, F. (2007). Inter-chromosomal gene regulation in the mammalian cell nucleus. Curr. Opin. Genet. Dev. *17*, 456–464.

Enoch, T., Zinn, K., and Maniatis, T. (1986). Activation of the human β-interferon gene requires an interferon-inducible factor. Mol. Cell. Biol. *6*, 801–810.

Escalante, C.R., Nistal-Villan, E., Shen, L., Garcia-Sastre, A., and Aggarwal, A.K. (2007). Structure of IRF-3 bound to the PRDIII-I element of the human interferon−βeta enhancer. Mol. Cell *26*, 703–716.

Guo, L., Hu-Li, J., and Paul, W.E. (2005). Probabilistic regulation in TH2 cells accounts for monoallelic expression of IL-4 and IL-13. Immunity *23*, 89–99.

Holländer, G.A., Zuklys, S., Morel, C., Mizoguchi, E., Mobisson, K., Simpson, S., Terhorst, C., Wishart, W., Golan, D.E., Bhan, A.K., and Burakoff, S.J. (1998). Monoallelic expression of the interleukin-2 locus. Science *279*, 2118–2121.

Honda, K., Takaoka, A., and Taniguchi, T. (2006). Type I interferon gene induction by the interferon regulatory factor family of transcription factors. Immunity *25*, 349–360.

Hottiger, M.O., Felzien, L.K., and Nabel, G.J. (1998). Modulation of cytokine-induced HIV gene expression by competitive binding of transcription factors to the coactivator p300. EMBO J. *17*, 3124–3134.

Hu, J., Sealfon, S.C., Hayot, F., Jayaprakash, C., Kumar, M., Pendleton, A.C., Ganee, A., Fernandez-Sesma, A., Moran, T.M., and Wetmur, J.G. (2007). Chromosome-specific and noisy IFNB1 transcription in individual virus-infected human primary dendritic cells. Nucleic Acids Res. *35*, 5232–5241.

Kelly, B.L., and Locksley, R.M. (2000). Coordinate regulation of the IL-4, IL-13, and IL-5 cytokine cluster in Th2 clones revealed by allelic expression patterns. J. Immunol. *165*, 2982–2986.

Ling, J.Q., Li, T., Hu, J.F., Vu, T.H., Chen, H.L., Qiu, X.W., Cherry, A.M., and Hoffman, A.R. (2006). CTCF mediates interchromosomal colocalization between Igf2/H19 and Wsb1/Nf1. Science *312*, 269–272.

Lipniacki, T., Paszek, P., Brasier, A.R., Luxon, B.A., and Kimmel, M. (2006). Stochastic regulation in early immune response. Biophys. J. *90*, 725–742.

Lomvardas, S., and Thanos, D. (2001). Nucleosome sliding via TBP DNA binding in vivo. Cell *106*, 685–696.

Lomvardas, S., and Thanos, D. (2002). Modifying gene expression programs by altering core promoter chromatin architecture. Cell *110*, 261–271.

Lomvardas, S., Barnea, G., Pisapia, D.J., Mendelsohn, M., Kirkland, J., and Axel, R. (2006). Interchromosomal interactions and olfactory receptor choice. Cell *126*, 403–413.

Maniatis, T., Falvo, J.V., Kim, T.H., Kim, T.K., Lin, C.H., Parekh, B.S., and Wathelet, M.G. (1998). Structure and function of the interferon–beta enhanceosome. Cold Spring Harb. Symp. Quant. Biol. *63*, 609–620.

Misteli, T. (2007). Beyond the sequence: cellular organization of genome function. Cell *128*, 787–800.

Munshi, N., Yie, Y., Merika, M., Senger, K., Lomvardas, S., Agalioti, T., and Thanos, D. (1999). The IFN–beta enhancer: a paradigm for understanding activation and repression of inducible gene expression. Cold Spring Harb. Symp. Quant. Biol. *64*, 149–159.

Munshi, N., Agalioti, T., Lomvardas, S., Merika, M., Chen, G., and Thanos, D. (2001). Coordination of a transcriptional switch by HMGI(Y) acetylation. Science *293*, 1133–1136.

Nelson, D.E., Ihekwaba, A.E., Elliott, M., Johnson, J.R., Gibney, C.A., Foreman, B.E., Nelson, G., See, V., Horton, C.A., Spiller, D.G., et al. (2004). Oscillations in NF–κappaB signaling control the dynamics of gene expression. Science *306*, 704–708.

Osborne, C., Chakalova, L., Brown, K.E., Carter, D., Horton, A., Debrand, E., Goyenechea, B., Mitchell, J.A., Lopes, S., Reik, W., and Fraser, P. (2004). Active genes dynamically colocalize to shared sites of ongoing transcription. Nat. Genet. *36*, 1065–1069.

Panne, D., Maniatis, T., and Harrison, S.C. (2007). An atomic model of the interferon–βeta enhanceosome. Cell *129*, 1111–1123.

Papatsenko, D., and Levine, M. (2007). A rationale for the enhanceosome and other evolutionarily constrained enhancers. Curr. Biol. *17*, R955–R957.

Paun, A., and Pitha, P.M. (2007). The innate antiviral response: new insights into a continuing story. Adv. Virus Res. *69*, 1–66.

Polak, P., and Domany, E. (2006). Alu elements contain many binding sites for transcription factors and may play a role in regulation of developmental processes. BMC Genomics *7*, 133.

Riviere, I., Sunshine, M.J., and Littman, D.R. (1998). Regulation of IL-4 expression by activation of individual alleles. Immunity *9*, 217–228.

Sato, M., Suemori, H., Hata, N., Asagiri, M., Ogasawara, K., Nakao, K., Nakaya, T., Katsuki, M., Noguchi, S., Tanaka, N., et al. (2000). Distinct and essential roles of transcription factors IRF-3 and IRF-7 in response to viruses for IFN-alpha/beta gene induction. Immunity *13*, 539–548.

Senger, K., Merika, M., Agalioti, T., Yie, J., Escalante, C.R., Chen, G., Aggarwal, A.K., and Thanos, D. (2000). Gene repression by coactivator repulsion. Mol. Cell *6*, 931–937.

Spilianakis, C.G., Lalioti, M.D., Town, T., Lee, G.R., and Flavell, R.A. (2005). Interchromosomal associations between alternatively expressed loci. Nature *435*, 637–645.

Stetson, D.B., and Medzhitov, R. (2006). Types I interferons in host defense. Immunity *25*, 373–381.

Taniguchi, T., and Takaoka, A. (2002). The interferon-alpha/beta system in antiviral responses: a multimodal machinery of gene regulation by the IRF family of transcription factors. Curr. Opin. Immunol. *14*, 111–116.

Thanos, D., and Maniatis, T. (1995). Virus induction of human IFN beta gene expression requires the assembly of an enhanceosome. Cell *83*, 1091–1100.

Wurtele, H., and Chartrand, P. (2006). Genome-wide scanning of HoxB1-associated loci in mouse ES cells using an open-ended Chromosome Conformation Capture methodology. Chromosome Res. *14*, 477–495.

Xu, N., Tsai, C.L., and Lee, J.T. (2006). Transient homologous chromosome pairing marks the onset of X inactivation. Science *311*, 1149–1152.

Zawatzky, R., De Maeyer, E., and De Maeyer-Guignard, J. (1985). Identification of individual interferon-producing cells by in situ hybridiazation. Proc. Natl. Acad. Sci. USA *82*, 1136–1140.

Zhao, Z., Tavoosidana, G., Sjolinder, M., Gondor, A., Mariano, P., Wang, S., Kanduri, C., Lezcano, M., Sandhu, K.S., Singh, U., et al. (2006). Circular chromosome conformation capture (4C) uncovers extensive networks of epigenetically regulated intra- and interchromosomal interactions. Nat. Genet. *38*, 1341–1347.